

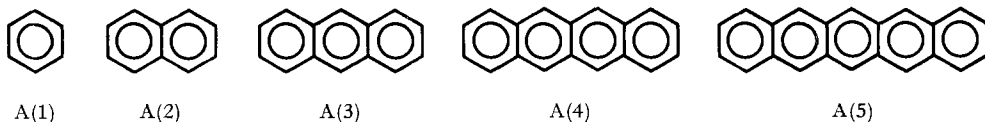
140. The  $\pi$ -Orbital Energies of the Acenes<sup>1)</sup>by Patricia A. Clark<sup>2)</sup>, F. Brogli and E. Heilbronner

Physikalisch-Chemisches Institut der Universität Basel

(17. IV. 72)

*Summary.* The 'observed'  $\pi$ -orbital energies  $\varepsilon_{v,j} = -I_{v,j}$  derived from the vertical ionization potentials obtained by a photoelectron spectroscopic investigation of the acenes benzene A(1), naphthalene A(2), anthracene A(3), naphthacene A(4) and pentacene A(5) have been compared with  $\pi$ -orbital energies calculated by three different approximations: (a) the standard *Hückel* HMO model; (b) a first-order perturbation treatment, based on (a), that takes into account bond length changes which follow the ionization process; (c) a SCF  $\pi$ -electron model of the type proposed by *Pople* and by *Pariser & Parr*. In agreement with previous experience it is found that model (b) yields the most satisfactory parametrization of the experimental data.

At least since the fundamental work of *Clar* [2] and his school on the higher acenes A(N) and on other benzenoid hydrocarbons, it has become obvious that the physical and chemical properties of these molecules are smooth, monotonic functions of the number N of annelated rings.



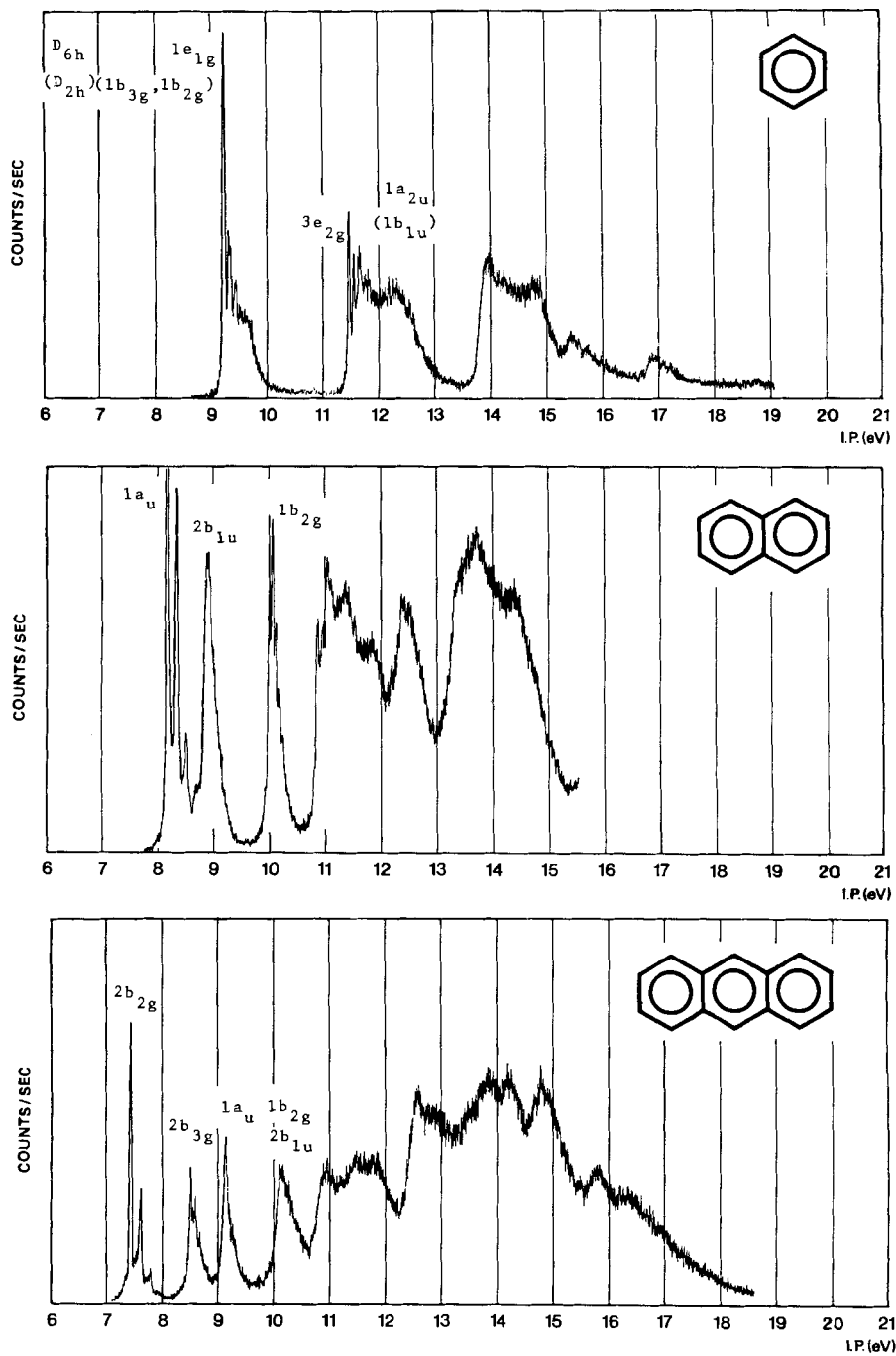
The comparison of the observed dependence on N of a given property (e.g. position and intensity of bands in the electronic spectra [3], first ionization potentials [4], polarographic reduction potentials [5], interatomic distances [6]) with the corresponding calculated dependence has been used as the touchstone for the predictive qualities of the various theoretical molecular orbital models used for description of the electronic structure of the  $\pi$ -systems of acenes and of 'aromatic' hydrocarbons in general.

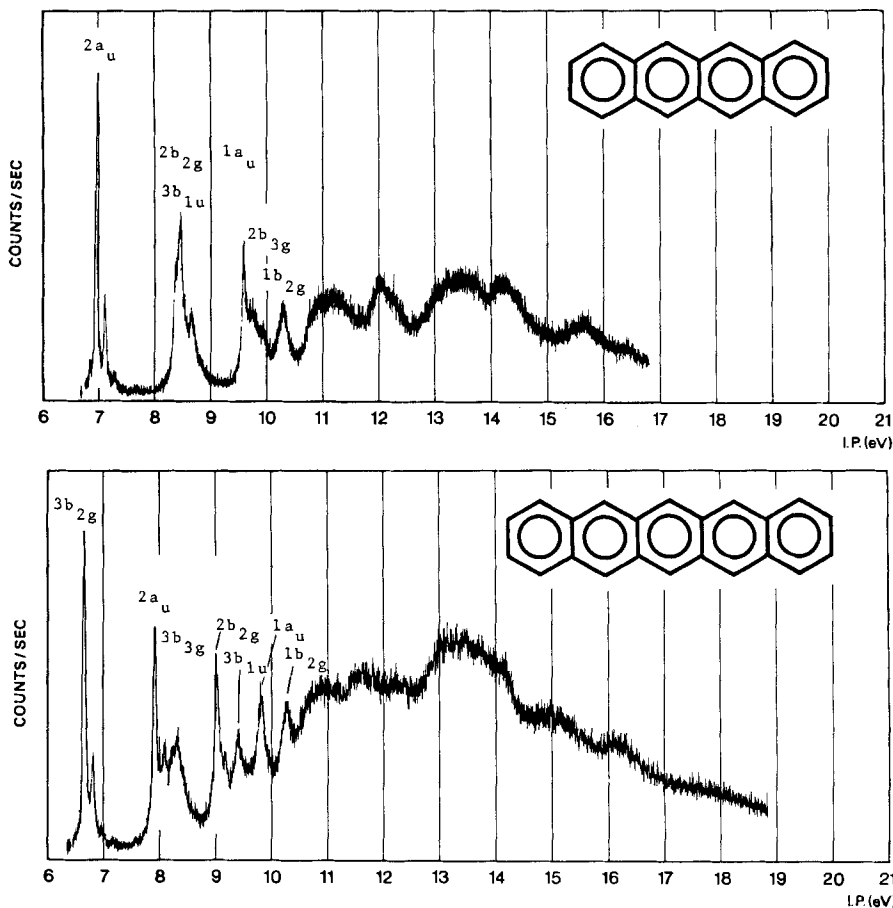
Concerning the early history of the calculation of molecular orbital energies for large  $\pi$ -systems, the reader is referred to the now classic treatise of *Pullman & Pullman* [7] and to the first tabulation of such values by *Coulson & Daudel* [8]. Summaries of more recent developments can be found in the books of *Streitwieser* [9], *Salem* [10] and *Dewar* [11].

Although molecular orbital energies for large  $\pi$ -systems have thus been known for some time [7] [12], they have so far escaped experimental verification, with the exception of the energies of the highest occupied (HOMO) and the lowest unoccupied (LUMO) molecular orbitals which can be correlated with first ionization potentials [4] or electron affinities [5]. With the advent of photoelectron (PE.) spectroscopy [13]

<sup>1)</sup> Part 37 of 'Applications of Photoelectron Spectroscopy'. Part 36: [1].

<sup>2)</sup> Permanent Address: Vassar College, Poughkeepsie, New York.




 Fig. 1. PE spectra of the acenes  $A(N)$ 

The labels refer to the orbitals given in Table 1. (Axes defined as shown in (4))

such a verification has now become possible for almost the whole set of  $\pi$ -orbital energies.

Koopmans has shown [14] that the self-consistent field (SCF) orbital energies  $\epsilon_j^{\text{SCF}}$  calculated for a closed shell molecule  $M$  in its electronic ground state

$$\Gamma \equiv (\psi_1)^2(\psi_2)^2 \dots (\psi_j)^2 \dots (\psi_{\text{HOMO}})^2 \quad (1)$$

yield directly the vertical ionization potentials  $I_{v,j}$  for the process leading to the radical cation  $M^+(\psi_j^{-1})$ :

$$I_{v,j} = -\epsilon_j^{\text{SCF}} \quad (2)$$

$I_{v,j}$  is the energy of the radical cation  $M^+$  with the same geometric structure as  $M$  and in the electronic state

$$\Psi_j = (\psi_1)^2(\psi_2)^2 \dots (\psi_j)^1 \dots (\psi_{\text{HOMO}})^2, \quad (3)$$

relative to the energy of M in state (1). Note that in (1) and (3) the orbitals  $\psi_i$  ( $i = 1, 2, \dots$  HOMO) are the SCF orbitals of groundstate M.

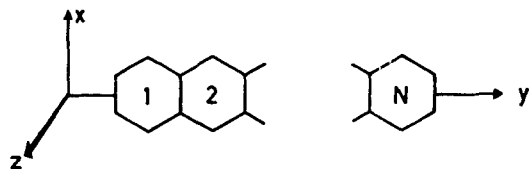
Although theorem (2) is subject to severe limitations due to neglect of changes in the orbitals  $\psi_i$  under the influence of the distribution of positive charge in  $M^+(\psi_j^{-1})$  and of the corresponding differences in correlation energies [15], it has proved a useful tool in PE.-spectroscopic investigations. It has become customary to equate observed vertical ionization potentials  $I_{v,j}$  with negative 'observed' orbital energies  $\varepsilon_{v,j} = -I_{v,j}$ .

We shall adhere to this convention in the present communication. Furthermore, we shall substitute in (2) for  $\varepsilon_j^{\text{SCF}}$  the orbital energies  $\varepsilon_j$  calculated from simple HMO models. A comparison of  $-I_{v,j}$  with  $\varepsilon_j$  provides a test for the quality of such models, which depend, in the last analysis, only on the connectivity pattern of the individual  $2p_z$ -AOs in the  $\pi$ -system as represented by the topological (*Hückel*) matrix. This approach implies the assumptions: (a) that in extended  $\pi$ -systems, such as those of the hydrocarbons A(N), the relative spacing of the *Hückel* molecular orbital energies  $\varepsilon_j$  is close to that of the SCF orbital energies  $\varepsilon_j^{\text{SCF}}$ ; (b) that the limitations inherent in (2) are less severe for molecules containing large  $\pi$ -systems than for small  $\sigma$ -bonded molecules.

Fig. 1 shows the PE. spectra of A(1) to A(5) recorded on a PS16 spectrometer of *Perkin-Elmer* Ltd. (Beaconsfield, England), provided with a high temperature inlet system and a heated target chamber. A(1) and A(2) were recorded at room temperature, the higher acenes at 100°C (A(3)), 175°C (A(4)) and 240°C (A(5)). The labels assigned to the bands refer to the convention summarized in (4), (6), (7) and (8). The corresponding vertical ionization potentials  $I_{v,j}$  are given in Table 1. For comparison we have included the  $\pi$ -ionization potentials previously reported by other authors for A(1), A(2) and A(3).

### Model: HMO

*Coulson* has shown [16] that in the framework of standard *Hückel*-MO theory [9] the  $4N+2$   $\pi$ -orbital energies of an N-acene A(N) can be obtained in closed form, i.e.



$$\varepsilon = \alpha + \beta; \alpha - \beta; \alpha + \frac{\beta}{2} \pm 1 \pm \sqrt{9 + 8 \cos(\pi J / (N + 1))}, \quad (4)$$

where  $J = 1, 2, \dots, N$ . Using the abbreviations  $\varepsilon = \alpha + x\beta$  and  $r_J = (9 + 8 \cos(\pi J / (N + 1)))^{1/2}$  the  $2N + 1$  bonding orbitals have energies determined by the coefficients

$$\varepsilon_j = \alpha + x_j \beta \begin{cases} x^0 = 1 \\ x_j^+ = (r_J + 1)/2 \\ x_j^- = (r_J - 1)/2 \end{cases} \quad (5)$$

The corresponding linear combinations  $\psi$  belong to the following irreducible representations of  $D_{2h}$ , if the axes are chosen as indicated in the diagram of formula (4):

$$\begin{array}{ll} N : \text{even} & \text{odd} \\ \psi^0 : B_{1u} & B_{3g} \end{array} \quad (6)$$

$$\begin{array}{ll} J : \text{even} & \text{odd} \\ \psi_J^+ : B_{3g} & B_{1u} \\ \psi_J^- : A_u & B_{2g} \end{array} \quad (7)$$

The correlation  $\varepsilon = \varepsilon(N, J)$ , which at first sight seems to be the 'natural' one, is that with  $J = N - K$ , where  $K$  is constant for each set of correlated orbitals, e.g.  $K = 0$  (or  $J = N$ ) for the set of the highest occupied  $\pi$ -orbitals (HOMO). However, as seen from (7) and from Fig. 2 (dotted line connecting the HOMOs), this type of correlation has the disadvantage that the orbitals in each set belong to two different irreducible representations.

Therefore we prefer to correlate the orbitals  $\psi_J^+$  or  $\psi_J^-$  with the same quantum number  $J$ , i.e.  $\varepsilon^+ = \varepsilon^+(N, J)$  and  $\varepsilon^- = \varepsilon^-(N, J)$  with  $J = \text{constant}$ , as indicated by the

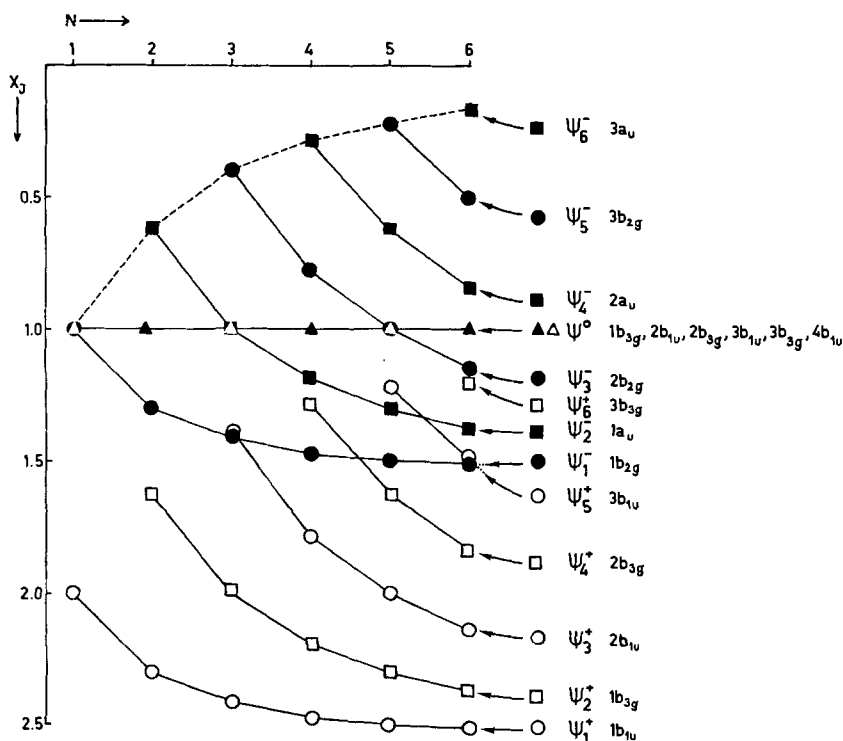


Fig. 2. Correlation diagram of the acene HMO orbital energies as given by Coulson's formula (4)

The definition of  $\psi_J^+$ ,  $\psi_J^-$  and  $\psi^0$  corresponds to that given in (5). The orbitals connected by solid lines carry the same label. With reference to (6) and (7) we have

$$\begin{array}{lll} \psi_J^+ & \psi_J^- & \psi^0 \\ \blacksquare A_u & \square B_{3g} & \circ B_{3u} \\ \bullet B_{2g} & \circ B_{1u} & \triangle B_{1g} \end{array}$$

The orbitals connected with a dotted line are the  $\psi_{\text{HOMO}}$ , i.e. the highest occupied  $\pi$ -orbitals of the  $A(N)$

solid lines in Fig. 2. In this fashion orbitals belonging to the same irreducible representation and having the same nodal properties are collected in the same set.

For the purpose of this correlation the  $\pi$ -orbitals of benzene belonging to  $A_{2u}$  and  $E_g$  of  $D_{6h}$  are written in the usual real form and classified as  $B_{1u}$ ,  $B_{2g}$  and  $B_{3g}$  relative to the lower symmetry group  $D_{2h}$ .

As is evident from (5) and from Fig. 2, the set of orbital energies  $\varepsilon_j^+$  and the set  $\varepsilon_j^-$  plotted as a function of  $N$  form the same pattern, the former being displaced downwards by  $2\beta$  relative to the latter. All orbitals  $\psi^0$  have  $\varepsilon^0 = \alpha + \beta$  and thus lie above the orbital energies  $\varepsilon_j^+$  for all  $N$  and  $J$  because of the relationship  $1 \leq r_j \leq \sqrt{17}$ . Accordingly the symmetry labels of the  $\pi$ -orbitals are uniquely definable as follows:

$$\begin{aligned}
 \psi_j^+ : J \text{ odd} & \left( \frac{J+1}{2} \right) \mathbf{b}_{1u} \\
 & J \text{ even} \left( \frac{J}{2} \right) \mathbf{b}_{3g} \\
 \psi_j^- : J \text{ odd} & \left( \frac{J+1}{2} \right) \mathbf{b}_{2g} \\
 & J \text{ even} \left( \frac{J}{2} \right) \mathbf{a}_u \\
 \psi^0 : N \text{ odd} & \left( \frac{N+1}{2} \right) \mathbf{b}_{3g} \\
 & N \text{ even} \left( \frac{N+2}{2} \right) \mathbf{b}_{1u}
 \end{aligned} \tag{8}$$

As mentioned above, a characteristic feature of the HMO model is that to every acene  $A(N)$  there is assigned an orbital  $\psi^0$  of energy  $\alpha + \beta$  (see (6)), which belongs to  $B_{1u}$  or  $B_{3g}$  depending on whether  $N$  is even or odd and which, for  $N$  odd, is accidentally degenerate with an orbital of the class  $\psi_j^+$  belonging to  $B_{2g}$  or  $A_u$  (see Fig. 2). These orbitals  $\psi^0$  are all modelled after the same pattern shown schematically in (9):

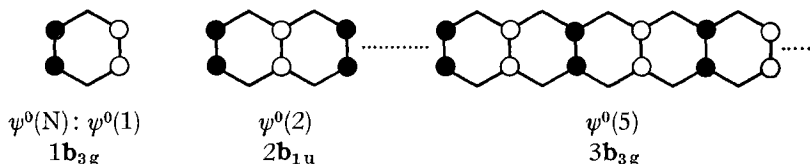


Fig. 3a shows the correlation diagram based on the 'observed' orbital energies  $\varepsilon_{v,j} = -I_{v,j}$ . While the general trend for the 'observed' energies of  $\psi_j^+$  and  $\psi_j^-$  corresponds closely to the one derived from the simple HMO model, there is one striking difference, namely, the increasing upward displacement of  $\varepsilon_v^0$  with increasing  $N$ , from  $\varepsilon_v^0 = -9.2_5$  eV for  $N = 1$  to  $\varepsilon_v^0 = -8.3_5$  for  $N = 5$ . As a consequence the accidental degeneracy of  $2\mathbf{b}_{3g}$  and  $1\mathbf{a}_u$  predicted for  $A(3)$  is lifted; the corresponding correlation lines cross near  $-8.7$  eV between  $N = 2$  and  $3$ . On the other hand a new near-degeneracy (inside the limits of experimental error) occurs for  $3\mathbf{b}_{1u}$  and  $2\mathbf{b}_{2g}$  of  $A(4)$  at

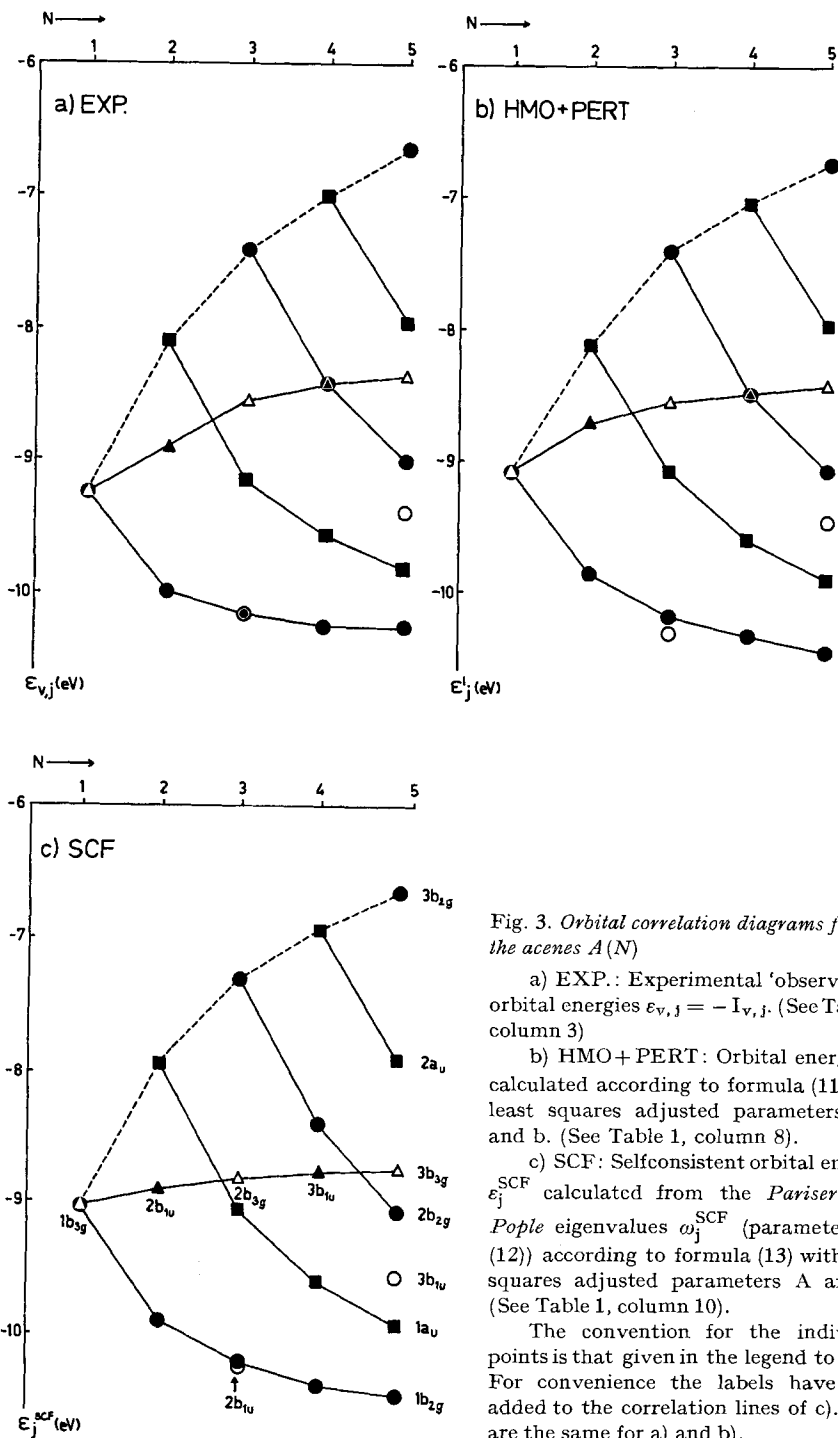


Fig. 3. Orbital correlation diagrams for the acenes  $A(N)$

a) EXP.: Experimental 'observed' orbital energies  $\varepsilon_{v,j} = -I_{v,j}$ . (See Table 1, column 3)

b) HMO+PERT: Orbital energies  $\varepsilon'_j$  calculated according to formula (11) with least squares adjusted parameters  $\alpha$ ,  $\beta$  and  $b$ . (See Table 1, column 8).

c) SCF: Selfconsistent orbital energies  $\varepsilon_j^{\text{SCF}}$  calculated from the Pariser-Parr-Pople eigenvalues  $\omega_j^{\text{SCF}}$  (parameters see (12)) according to formula (13) with least squares adjusted parameters  $A$  and  $B$ . (See Table 1, column 10).

The convention for the individual points is that given in the legend to Fig 2. For convenience the labels have been added to the correlation lines of c). They are the same for a) and b).

– 8.4 eV, which is absent in the HMO results. Finally the degeneracy of  $3b_{3g}$  and  $2b_{2g}$  calculated for A(5) is again lifted, the experimentally found difference in 'observed' orbital energies being  $\sim 0.6$  eV.

**Model: HMO including corrections for ionization-induced bond-length changes.**

As pointed out in a previous communication [17] the major error in applying the standard HMO technique to the calculation of PE. spectroscopic data of  $\pi$ -systems consists in the neglect of the change in equilibrium bond lengths  $\Delta R_{\mu\nu, j} = R_{\mu\nu, j}^+ - R_{\mu\nu}$

Table 1. *Experimental and calculated vertical ionization potentials of the acenes A(N)*  
The values given in columns 3, 6, 8 and 10 are in eV

Column 1: Acene A(N)

Column 2: Orbital label; symmetry group  $D_{2h}$ ; axes oriented as shown in (4)

Column 3: Vertical ionization potentials; these refer to the vibrational component of highest intensity (*Franch-Condon* factor); Values in brackets are uncertain due to overlap with bands of higher intensity

Column 4: Ionization potentials previously given in the literature

Column 5: Coefficients for orbital energies  $\epsilon_j = \alpha + x_j\beta$  from standard HMO theory. (See formula (5))

Column 6: Orbital energies obtained from a (least squares) regression of  $I_{v, j}$  on  $x_j$

Column 7: Perturbation term calculated according to (10)

Column 8: Orbital energies obtained from a (least squares) regression based on formula (11)

Column 9: *Pariser-Parr-Pople* SCF eigenvalues calculated with the parameters given in (12)

Column 10: Orbital energies obtained from a (least squares) regression based on formula (13)

1	2	3	4	5		6		7		8		9		10	
				$x_j$	$-\epsilon_j$	$Y_j$	$-\epsilon_j'$	$\omega_j^{\text{SCF}}$	$-\epsilon_j^{\text{SCF}}$						
		$I_{v, j}$ (ineV)	Ref.		HMO	HMO+ PERT.		SCF							
	$\psi_j$				$x_j$	$-\epsilon_j$	$Y_j$	$-\epsilon_j'$	$\omega_j^{\text{SCF}}$	$-\epsilon_j^{\text{SCF}}$					
A(1)	$1b_{3g}^a$	9.24	[22]		1.000	8.98	0.000	9.06	0.8005	9.03					
	$1b_{2g}^a$	9.24			1.000	8.98	0.000	9.06	0.8005	9.03					
	$1b_{1u}^a$	12.25			2.000	11.89	0.000	12.25	-2.0952	11.88					
A(2)	$1a_u$	8.15	8.12 [26]; 8.11 [27]		0.618	7.87	0.035	8.11	1.9146	7.93					
	$2b_{1u}$	8.88	8.90 8.79		1.000	8.98	-0.046	8.70	0.9384	8.89					
	$1b_{2g}$	10.10	10.00 9.96		1.303	9.86	-0.024	9.84	-0.0816	9.90					
A(3)	$2b_{2g}$	7.40	7.41 [28]		0.414	7.28	0.026	7.39	2.5575	7.30					
	$2b_{3g}$	8.52	8.55		1.000	8.98	-0.066	8.54	1.0150	8.82					
	$1a_u$	9.16	9.16		1.000	8.98	0.001	9.07	0.7844	9.04					
	$1b_{2g}$	10.13	10.16		1.414	10.18	-0.029	10.16	-0.3950	10.21					
	$2b_{1u}$	10.21			1.414	10.18	-0.013	10.28	-0.4117	10.22					
A(4)	$2a_u$	7.01 <sup>b)</sup>	6.95 [29] [30]		0.295	6.93	0.030	7.04	2.9511	6.91					
	$2b_{2g}$	8.41			0.778	8.34	0.014	8.46	1.4466	8.39					
	$3b_{1u}$	(8.6)			1.000	8.98	-0.076	8.46	1.0611	8.77					
	$1a_u$	9.56			1.194	9.55	-0.013	9.58	0.2172	9.60					
	$2b_{3g}$	(9.7)			1.295	9.84	-0.028	9.78	0.0030	9.81					
	$1b_{2g}$	10.25			1.467	10.34	-0.032	10.30	-0.5673	10.38					
A(5)	$3b_{2g}$	6.64	6.23 [30] [31]		0.220	6.71	0.024	6.76	3.2163	6.65					
	$2a_u$	7.93			0.618	7.87	0.018	7.98	1.9379	7.91					
	$3b_{8g}$	8.35			1.000	8.98	-0.083	8.41	1.0908	8.74					
	$2b_{2g}$	9.00			1.000	8.98	-0.002	9.05	0.7821	9.05					
	$3b_{1u}$	9.39			1.220	9.62	-0.041	9.44	0.2704	9.55					
	$1a_u$	9.80			1.303	9.86	-0.020	9.87	-0.1000	9.92					
	$1b_{2g}$	10.26			1.496	10.42	-0.029	10.42	-0.6525	10.46					

<sup>a)</sup> Classification of the orbitals in real representation relative to  $D_{2h}$  with axes as defined in (4).

<sup>b)</sup> These values have been reported previously in [1].



which follows the vertical ionization process  $M + h\nu \rightarrow M^+(\psi_j^{-1}) + e$ . Here  $R_{\mu\nu}^+$  and  $R_{\mu\nu}$  are the lengths of the bond  $\mu, \nu$  in  $M^+(\psi_j^{-1})$  and  $M$  respectively. The necessary correction  $\delta\varepsilon_j$  can be estimated from the changes in bond order  $p_{\mu\nu}$  on removal of an electron from orbital  $\psi_j$ , by a simple first-order perturbation treatment [18]:

$$\delta\varepsilon_j = by_j = b \sum_{\mu\nu} (p_{\mu\nu}^+ - p_{\mu\nu}) (p_0 - p_{\mu\nu}). \quad (10)$$

Here  $p_{\mu\nu}$  is the bond order of the bond  $\mu\nu$  in  $M$ ,  $p_{\mu\nu}^+$  in  $M^+(\psi_j^{-1})$  and  $p_0 = 2/3$  the bond order for a  $\pi$ -bond of standard length  $R_0 = 1.39 \text{ \AA}$ , i.e. in A(1). The constant  $b$  depends on the force constants of an  $sp^2$ - $sp^2$  single bond and of a double bond of length  $R_0$ , as well as on the derivative  $d\beta/dR$  of the resonance integral. In practice  $b$  is handled as an adjustable parameter [17], [18] (see also [1]). Table 1 contains the

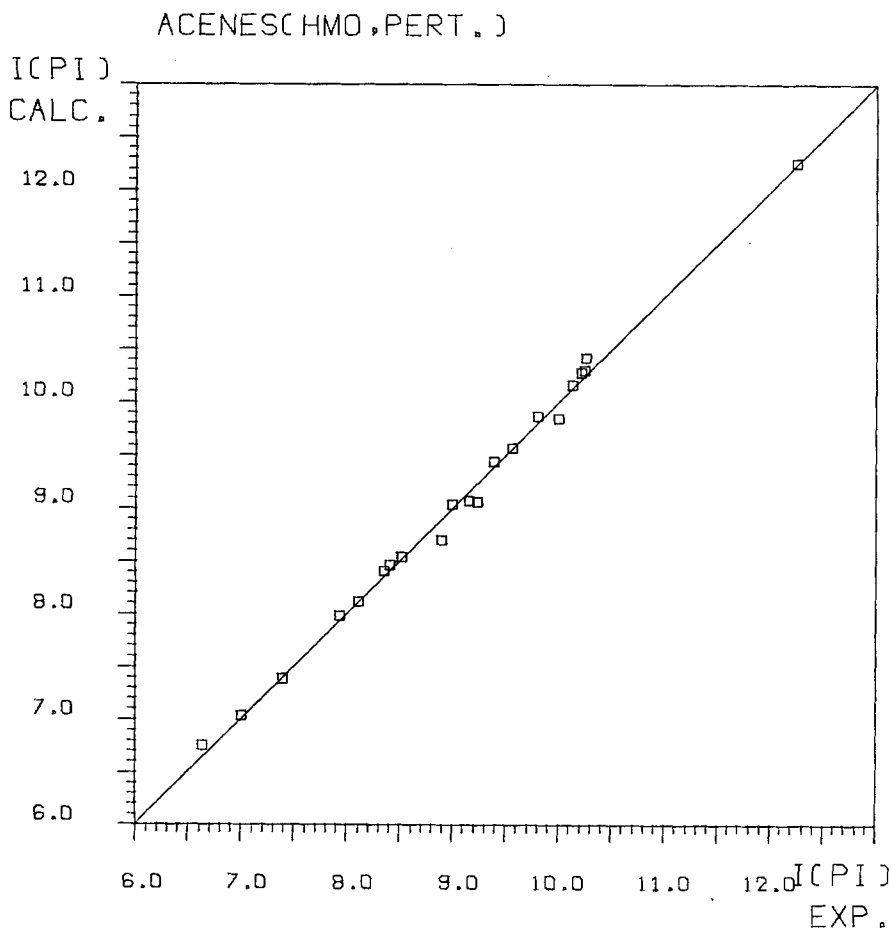


Fig. 4. Computer drawn regression  $I_{v,j}$  ( $= I(PI) \text{ EXP.}$ ) vs.  $\varepsilon_j'$  ( $= I(PI) \text{ CALC.}$ )  
The latter values have been calculated from formula (11) with least squares adjusted parameters  $\alpha$ ,  $\beta$  and  $b$

parameters  $y_j$  calculated according to (10) and the orbital energies  $\epsilon'_j$  obtained by combining (5) and (10),

$$\epsilon'_j = \alpha + \beta \cdot x_j + b \cdot y_j, \quad (11)$$

and by subjecting (11) to a least squares treatment. The latter yields the following 90 percent confidence limits:  $\alpha = (-5.864 \pm 0.110)$  eV,  $\beta = (-3.196 \pm 0.107)$  eV and  $b = (-7.859 \pm 1.475)$  eV; residual variance about the regression  $V(\epsilon_j) = 0.0109$  eV<sup>2</sup>, corresponding to a standard error of  $SE(\epsilon_j) = 0.104$  eV. (For comparison [17]:  $\alpha = -5.85$  eV,  $\beta = -3.33$  eV and  $b = -7.73$  eV.)

The remarkable agreement between the observed ( $I_{v,j}$ ) and calculated ( $I'_j = -\epsilon'_j$ ) ionization potentials is evident from the data given in Table 1, the regression shown in Fig. 4 and the correlation diagram of Fig. 3b. Apart from the general numerical precision, the most gratifying feature is that our perturbation model explains satisfactorily the observed upwards trend of  $\epsilon^0$  as a function of  $N$ . Indeed, as expected from the character of the orbitals  $\psi^0$  shown in (8) and as can be seen from the values  $y_j$  contained in Table 1, the  $\epsilon^0$  values are those affected with the largest corrections  $\delta\epsilon_j$  for each system  $A(N)$ . Furthermore the magnitude of  $\delta\epsilon^0$  increases with increasing  $N$ : 0.000,  $N = 1$ ;  $-0.046$ ,  $N = 2$ ;  $-0.066$ ,  $N = 3$ ;  $-0.076$ ,  $N = 4$ ;  $-0.083$ ,  $N = 5$ . Note that the observed accidental degeneracy of  $3b_{1u}$  and  $2b_{2g}$  for  $A(4)$  is reproduced.

Previous calculations based on formula (11) have shown that the correction (10) leads to an equally striking improvement of the predicted  $\pi$ -orbital energies for linear unsaturated, non-alternant and non-benzenoid hydrocarbons [17] and for the five isomeric benzenoid molecules  $C_{18}H_{12}$  [1]. In contrast, a correction for the uneven distribution of the excess positive charge in  $M^+(\psi_j^{-1})$ , (e.g. by a first-order perturbation treatment) does not yield a further significant improvement of the  $\epsilon'_j$  values.

#### Model: SCF

It seemed of interest to investigate whether the discrepancies between the results of a simple HMO treatment ( $\epsilon_j$ ) and the experimental data ( $\epsilon_{v,j}$ ) can be removed by a self-consistent field calculation, i.e. by taking electron-electron interaction into account. The SCF method used is the one described by *Pople* [19] and by *Pariser & Parr* [20] (neglecting configuration interaction). To ensure a straightforward comparison with the simple HMO results, we assume all bonds of equal length, i.e.  $R_0 = 1.397$  Å and all angles  $120^\circ$ . The parameters used are [21]:

$$\begin{aligned} \beta_{\mu\nu}^c &= -2.371 \text{ eV;} \\ \gamma_{\mu\mu} &= 10.959 \text{ eV;} \gamma_{\mu\nu} \text{ (bonded)} = 6.783 \text{ eV} \\ \gamma_{\mu\nu} (R \leq 6 \text{ \AA}; \text{ not bonded}) &= \frac{328.77 + R_{\mu\nu}}{30.0 + 12.341 R_{\mu\nu} + R_{\mu\nu}^2} \text{ eV} \\ \gamma_{\mu\nu} (R > 6 \text{ \AA}) &= 14.395/R_{\mu\nu} \text{ eV} \end{aligned} \quad (12)$$

The orbital energies  $\omega_j^{\text{SCF}}$  so obtained (relative to the energy of the basis  $2p_z$  - AOs) are given in Table 1. A least-squares calculation based on the linear regression function

$$\epsilon_j^{\text{SCF}} = A + B\omega_j^{\text{SCF}} \quad (13)$$

yields the following 90 percent confidence limits:  $A = (-9.816 \pm 0.078)$  eV,  $B = (0.984 \pm 0.054)$  eV, i.e. not significantly different from unity; residual variance about

the regression  $V(\epsilon_{v,j}) = 0.0325 \text{ eV}^2$ , corresponding to a standard error of  $SE(\epsilon_{v,j}) = 0.183 \text{ eV}$ . The residual variance is thus significantly greater than the one found by the perturbation treatment:  $F = 0.0325/0.0109 = 2.98$  as compared to  $F = 2.2$  for 95 percent security and 18 degrees of freedom for both variances. As can be seen from the correlation diagram of Fig. 3c, the inclusion of electron interaction also tends to shift  $\psi^0$  towards higher orbital energies with increasing  $N$ . However, this interaction accounts for only a third of the observed effect, and we are led to the conclusion that the major part of the observed displacement is due to the change  $\Delta R_{\mu\nu}$  in interatomic distances, i.e. to the perturbation  $\delta\epsilon_j$  given in (10).

The overall agreement between  $\epsilon_j^{\text{SCF}}$  (from (13)) and  $\epsilon_{v,j}$  is shown in Fig. 5.

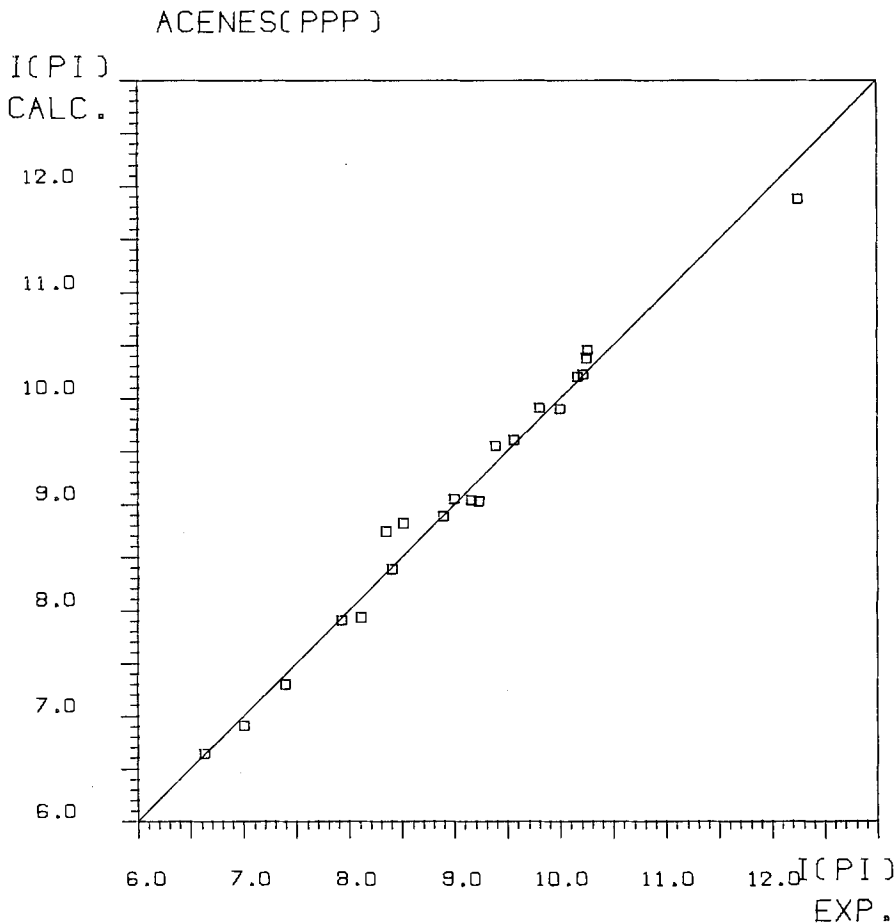


Fig. 5. Computer drawn regression of  $I_{v,j} (= I(PI) \text{ EXP})$  vs.  $\epsilon_j^{\text{SCF}} (= I(PI) \text{ CALC})$ . The latter values have been calculated from formula (13) with least squares adjusted parameters A and B

### Remarks

1. The calibration of formula (11), which relies on 18 degrees of freedom, yielded values for the parameters  $\alpha$ ,  $\beta$  and  $b$  which did not differ significantly from those

obtained previously [1], [17]. Consequently we are in a position to assign rather reliable confidence limits to unknown or uncertain  $\pi$ -ionization potentials, e.g. the lower  $I_{v,j}$  values of the acenes A(2) to A(5) or the set of  $I_{v,j}$  values of A(6). Such values have been collected in Table 2.

Table 2. *Low-lying  $\pi$ -orbital energies of the acenes A(N)*

	$\psi_j$	$-\varepsilon_{v,j}$ = $I_{v,j}$	$x_j$	$-\varepsilon_j^a)$	$y_j$	$-\varepsilon_j^b)$	$\omega_j^{\text{SCF}}$	$-\varepsilon_j^{\text{SCF}e)}$
A(2)	<b>1b<sub>3g</sub></b>	10.86	1.618	10.77 ± 0.44	0.003	11.06 ± 0.20	-1.0240	10.82 ± 0.33
	<b>1b<sub>1u</sub></b>	d)	2.303	12.77 ± 0.50	-0.084	12.57 ± 0.22	-2.8257	12.60 ± 0.37
A(3)	<b>1b<sub>3g</sub></b>	11.9	2.000	11.89 ± 0.47	-0.064	11.75 ± 0.21	-2.0079	11.79 ± 0.35
	<b>1b<sub>1u</sub></b>	12.64	2.414	13.09 ± 0.51	-0.112	12.70 ± 0.24	-3.0995	12.87 ± 0.38
A(4)	<b>2b<sub>1u</sub></b>	e)	1.778	11.24 ± 0.45	-0.058	11.09 ± 0.20	-1.3775	11.17 ± 0.34
	<b>1b<sub>3g</sub></b>	12.0	2.194	12.45 ± 0.49	-0.094	12.14 ± 0.22	-2.5094	12.29 ± 0.36
	<b>1b<sub>1u</sub></b>	e)	2.467	13.25 ± 0.52	-0.125	12.77 ± 0.24	-3.2289	12.99 ± 0.38
A(5)	<b>2b<sub>3g</sub></b>	e)	1.618	10.77 ± 0.44	-0.058	10.58 ± 0.20	-0.9004	10.70 ± 0.33
	<b>2b<sub>1u</sub></b>	e)	2.000	11.89 ± 0.47	-0.085	11.59 ± 0.21	-1.9745	11.76 ± 0.35
	<b>1b<sub>3g</sub></b>	e)	2.303	12.77 ± 0.50	-0.110	12.36 ± 0.23	-2.7929	12.57 ± 0.37
	<b>1b<sub>1u</sub></b>	e)	2.496	13.33 ± 0.52	-0.131	12.81 ± 0.24	-3.2999	13.06 ± 0.39

a) Calculated according to  $\varepsilon_j = \alpha + \beta x_j$  with  $\alpha = -(6.074 \pm 0.234)$  eV,  $\beta = -(2.907 \pm 0.210)$  eV. (90% confidence limits).

b) Calculated from formula (11) with the least squares parameters  $\alpha = -(5.864 \pm 0.100)$  eV,  $\beta = -(3.196 \pm 0.107)$  eV,  $b = -(7.859 \pm 1.475)$  eV. (90% confidence limits).

c) Calculated from (13) with  $A = -(9.816 \pm 0.078)$  eV,  $B = (0.984 \pm 0.054)$  eV. (90% confidence limits).

d) This orbital could be the one corresponding to the double band at 12.36 and 12.5 eV.

e) The corresponding  $\pi$ -bands are strongly overlapped by  $\sigma$ -bands (see Figure 1).

2. In the case of benzene A(1) the 90 percent confidence limits for the second  $\pi$ -ionization potential, corresponding to ejection of an electron from **1a<sub>2u</sub>** (in  $D_{6h}$ ; classified as **1b<sub>1u</sub>** relative to the sub-group  $D_{2h}$ ), are 12.05 and 12.49 eV. This confirms nicely the assignment proposed by *Lindholm* and his coworkers [22] for the PE. spectrum of A(1).

3. The comparison of the  $\varepsilon_j'$ -values obtained from formula (11) with the 'observed' values  $\varepsilon_{v,j} = -I_{v,j}$ , as shown in Fig. 4, indicates that the regression is *linear in  $x_j$*  with no significant quadratic component. The simple HMO treatment thus yields orbital energies appropriate for a correct description of the PE. bands of unsaturated hydrocarbons corresponding to  $\pi$ -ionization processes.

The correction for a fixed overlap integral  $S_{\mu\nu}$  between nearest neighbour atomic orbitals introduced some time ago by *Wheland* [23] does not yield a correlation of the same quality. The independent variable  $x_j'$ , to be used instead of  $x_j$  in formula (11), is defined as

$$x_j' = x_j / (1 + S_{\mu\nu} x_j) \quad (14)$$

with  $S_{\mu\nu} = 0.25$ . As a result, a curve of the type

$$\varepsilon_j'' = \alpha + \gamma x_j' + b y_j \quad (15)$$

passing through the points  $\varepsilon_j'' = -6.64$  eV for **3b<sub>2g</sub>** of A(5) and  $\varepsilon_j'' = -12.25$  eV for **1b<sub>1u</sub>** of A(1) (see correlation of Fig. 4) would be in error by about 0.6 eV in the region

$\varepsilon_j^* \approx -8$  to  $-10$  eV. This is roughly six times the standard error observed for the regression based on the standard *Hückel* approximation. We conclude that the once popular *Wheland*-correction is to be avoided when the HMO model is used for interpretation of PE. spectroscopic data of unsaturated hydrocarbons or of other molecules containing  $\pi$ -systems.

4. Once the  $\pi$ -bands have been identified in the PE. spectra of the acenes, the onset of the strongly overlapping  $\sigma$ -bands can be determined: A(1): 11.4 eV [22]; A(2): 11.4 eV; A(3):  $\sim 11.0$  eV; A(4):  $\sim 10.9$  eV; A(5):  $\sim 10.8$  eV.

5. The vibrational fine structure of the first band in the PE. spectra of the acenes A(N) with  $N > 1$  (benzene A(1) is a special case in view of its high symmetry; see [22]) shows a dominant progression with the following spacing:

A(2) Orbital:	$1a_u$	$\tilde{\nu}(\text{cm}^{-1})$ :	$\sim 1370$	
A(3)	$2b_{2g}$		$1380 \pm 90$	(16)
A(4)	$2a_u$		$1380 \pm 80$	
A(5)	$3b_{2g}$		$1300 \pm 110$	

In all these cases the photoelectron vacates the highest occupied orbital  $\psi_{\text{HOMO}}$ . The observed invariance of  $\tilde{\nu}$  with respect to N is in agreement with earlier electronic spectral results for the  ${}^1L_a \leftarrow {}^1A$  transition, i.e. the transition to an excited state involving mainly the singly excited configuration with  $\psi_{\text{HOMO}}$  and  $\psi_{\text{LUMO}}$  singly occupied: A(3):  $\tilde{\nu} = 1400 \text{ cm}^{-1}$ ; A(4):  $\tilde{\nu} = 1410 \text{ cm}^{-1}$ ; A(5):  $\tilde{\nu} = 1380 \text{ cm}^{-1}$  [24]. Because of the alternancy of A(N) [25],  $\psi_{\text{HOMO}}$  and  $\psi_{\text{LUMO}}$  differ only in the sign of the starred set of atomic orbitals. Consequently the change  $\Delta p_{\mu\nu}^*$  in bond order on electronic excitation to the  ${}^1L_a$  state is always exactly twice the change  $\Delta p_{\mu\nu}^+$  on ionization, and therefore the normal mode stimulated in both processes must be the same. It follows that the explanation given by *Murrell* [24] for the constancy of  $\tilde{\nu}$  in the vibrational fine structure of the acene  ${}^1L_a$  band is also valid for the first  $\pi$ -band in the PE. spectra.

The relationship  $\Delta p_{\mu\nu}^* = 2 \cdot p_{\mu\nu}^+$  would imply that the frequencies listed in (16) should be smaller than those derived from the  ${}^1L_a$  bands. This seems to be the case: from PE. spectra:  $\tilde{\nu} \approx 1350 \text{ cm}^{-1}$ ; from electronic spectra:  $\tilde{\nu} \approx 1400 \text{ cm}^{-1}$ . However, this result is not conclusive in view of the experimental uncertainties in the PE. spectroscopic data.

For the PE. bands at higher ionization potentials one finds: A(3):

A(3)	$2b_{3g}$	$\tilde{\nu}$ :	$710 \pm 40$ ; $410 \pm 100 \text{ cm}^{-1}$	
	$1a_u$		$1320 \pm 50 \text{ cm}^{-1}$	(17)
A(5)	$2a_u$		$1320 \pm 40 \text{ cm}^{-1}$	

We wish to thank Dr. *J. H. D. Eland* for having made his results available to us prior to publication.

This work is part of project Nr. SR 2.477.71 of the *Schweizerischer Nationalfonds*. Support by *CIBA-GEIGY S.A.* (Basel) is gratefully acknowledged.

*P. A. C.* is indebted to *Vassar College* for a leave of absence and *F. B.* thanks the *Kanton Aargau* for the grant of a fellowship.

## BIBLIOGRAPHY

- [1] *F. Brogli & E. Heilbronner*, *Angew. Chem.*, in print.
- [2] *E. Ciar*, 'Aromatische Kohlenwasserstoffe', *Springer Verlag*, Berlin 1941.
- [3] *H. B. Klevens & J. R. Platt*, *J. chem. Physics* 17, 470 (1949); *J. R. Platt*, *ibid.* 17, 484 (1949).
- [4] *A. Streitwieser, Jr. & P. M. Nair*, *Tetrahedron* 5, 149 (1959); *A. Streitwieser, Jr.*, *J. Amer. chem. Soc.* 82, 4123 (1960).
- [5] *A. Maccoll*, *Nature* 163, 178 (1949); *L. E. Lyons*, *ibid.* 166, 193 (1950); *A. Pullman, B. Pullman & G. Berthier*, *Bull. soc. chim. France* 17, 591 (1950).
- [6] *C. A. Coulson*, *Proc. Roy. Soc. A* 169, 413 (1939); *ibid.* A 207, 91 (1951); *J. Phys. Chem.* 56, 311 (1952).
- [7] *B. Pullman & A. Pullman*, 'Les Théories Electroniques de la Chimie Organique', *Masson et Cie.*, Paris, 1952.
- [8] *C. A. Coulson & R. Daudel*, 'Dictionnaire des Grandeurs Théoriques Descriptives des Molécules', Centre National de la Recherche Scientifique.
- [9] *A. Streitwieser, Jr.*, 'Molecular Orbital Theory for Organic Chemists', *J. Wiley & Sons*, New York 1961.
- [10] *L. Salem*, 'The Molecular Orbital Theory of Conjugated Systems', *W. A. Benjamin Inc.*, New York, 1966.
- [11] *M. J. S. Dewar*, 'The Molecular Orbital Theory of Organic Chemistry', *McGraw-Hill Comp.*, New York 1969.
- [12] *A. Streitwieser, Jr.*, & *J. I. Brauman* 'Supplement Tables of Molecular Orbital Calculations', *Pergamon Press*, Oxford, 1965; *E. Heilbronner & P. A. Straub*, 'HMO, Hückel Molecular Orbitals', *Springer Verlag* Berlin, 1966.
- [13] *D. W. Turner, C. Baker, A. D. Baker & C. R. Brundle*, 'Molecular Photoelectron Spectroscopy', *Wiley-Interscience*, London, 1970.
- [14] *T. Koopmans*, *Physica* 1, 104 (1934).
- [15] *M. Kotani, K. Ohno & K. Kayama*, *Handbuch der Physik*, Vol. XXXVII/2, p. 47, 53, *Springer Verlag*, Berlin, 1961; *W. G. Richards*, *J. Mass Spectrom. Ion Physics* 2, 419 (1969); see also [10] p. 156.
- [16] *C. A. Coulson*, *Proc. Phys. Soc.* 60, 257 (1948).
- [17] *F. Brogli & E. Heilbronner*, *Theoret. Chim. Acta*, in print.
- [18] *H. Götz & E. Heilbronner*, *Helv.* 44, 1365 (1961).
- [19] *J. A. Pople*, *Trans. Faraday Soc.* 49, 1375 (1953).
- [20] *R. Pariser & R. G. Parr*, *J. chem. Physics* 21, 466 (1953); *R. Pariser*, *ibid.* 24, 250 (1956); *R. G. Parr*, 'Quantum Theory of Molecular Electronic Structure', *W. A. Benjamin Inc.*, New York 1963.
- [21] *J. P. Weber*, Thesis Nr. 3856, Federal Institute of Technology, Zürich, Switzerland, 1966.
- [22] *L. Åsbrink, O. Edqvist, E. Lindholm & L. E. Selin*, *Chem. Physics Letters* 5, 192 (1970).
- [23] *G. W. Wheland*, *J. Amer. chem. Soc.* 63, 2025 (1941).
- [24] *J. N. Murrell*, 'The Theory of the Electronic Spectra of Organic Molecules', *Methuen & Co. Ltd.* London, 1963.
- [25] *C. A. Coulson & G. S. Rushbrooke*, *Proc. Cambridge Phil Soc.* 36, 193 (1940).
- [26] *J. H. D. Eland & C. J. Danby*, *Z. Naturforschung* 23a, 355 (1968).
- [27] *M. J. S. Dewar & S. D. Worley*, *J. Chem. Physics* 51, 263 (1969).
- [28] *J. H. D. Eland*, private communication.
- [29] *M. E. Wachs*, *J. Chem. Physics* 41, 1661 (1964).
- [30] *W. J. Wedenejew, L. W. Gurwitsch, W. H. Kondratjew, W. A. Medwedew & E. L. Frankewitsch*, 'Energien chemischer Bindungen, Ionisationspotentiale und Elektronenaffinitäten', *VEB Deutscher Verlag für Grundstoffindustrie*, Leipzig, 1971.
- [31] *R. M. Hedges & F. A. Matsen*, *J. Chem. Physics* 28, 950 (1958).
-